CORA Cork Open Research Archive
Cartlann Taighde Oscailte Chorcaí

Title	A study on the effects of damage models and wavelet bases for damage identification and calibration in beams
Authors	Pakrashi, Vikram;O'Connor, Alan J.;Basu, Biswajit
Publication date	2007-11-01
Original Citation	Pakrashi, V., O'Connor, A. and Basu, B. (2007), A Study on the Effects of Damage Models and Wavelet Bases for Damage Identification and Calibration in Beams. Computer-Aided Civil and Infrastructure Engineering, 22: 555–569. doi: 10.1111/j.1467-8667.2007.00510.x
Type of publication	Article (peer-reviewed)
Link to publisher's version	http://onlinelibrary.wiley.com/doi/10.1111/j.1467-8667.2007.00510.x/abstract - 10.1111/j.1467-8667.2007.00510.x
Rights	© 2007 Computer-Aided Civil and Infrastructure Engineering
Download date	2026-11-15 16:25:22
Item downloaded from	https://hdl.handle.net/10468/295



UCC
University College Cork, Ireland
Coláiste na hOllscoile Corcaigh


ucc
Coláiste na hOllscoile Corcaigh, Éire
University College Cork, Ireland

CORA
Cork Open Research Archive
Cartlann Taighde Oscailte Chorcaí

Pakrashi, V., O'Connor, A. and Basu, B. (2007), A Study on the Effects of Damage Models and Wavelet Bases for Damage Identification and Calibration in Beams. Computer-Aided Civil and Infrastructure Engineering, 22: 555–569. doi: 10.1111/j.1467-8667.2007.00510.x
http://onlinelibrary.wiley.com/doi/10.1111/j.1467-8667.2007.00510.x/abstract

The definitive version is available at www.blackwell-synergy.com

CORA Cork Open Research Archive http://cora.ucc.ie

A Study on the Effects of Damage Models and Wavelet Bases for Damage Identification and Calibration in Beams

Vikram Pakrashi, Alan O' Connor* and Biswajit Basu

Department of Civil, Structural and Environmental Engineering, Trinity College Dublin, Ireland

Abstract: *Damage detection and calibration in beams by wavelet analysis involve some key factors such as the damage model, the choice of the wavelet function, the effects of windowing and the effects of masking due to the presence of noise during measurement. A numerical study has been performed in this paper addressing these issues for single and multispan beams with an open crack. The first natural modeshapes of single and multispan beams with an open crack have been simulated considering damage models of different levels of complexity and analyzed for different crack depth ratios and crack positions. Gaussian white noise has been synthetically introduced to the simulated modeshape and the effects of varying signal to noise ratio have been studied. The wavelet based damage identification technique has been found to be simple, efficient and independent of damage models and wavelet basis functions, once certain conditions regarding the modeshape and the wavelet bases are satisfied. The wavelet based damage calibration is found to be dependant on a number of factors including damage models and the basis function used in the analysis. A calibration based on curvatures is more sensitive than a modeshape based calibration of the extent of damage.*

KEY WORDS: Wavelet, Open Crack, Signal to Noise Ratio, Windowing, Damage Modelling, Damage Calibration

Correspondence to: Dr. Alan O' Connor, Department of Civil, Structural and Environmental Engineering, Trinity College Dublin, Ireland

E-mail: alan.oconnor@tcd.ie

1. INTRODUCTION

The importance of structural health monitoring and damage detection of structures has increased significantly in recent times. A major focus in this field is the successful detection of the presence, location and the extent of damage present in a structure through new methodologies. Identification of damage in a freely vibrating beam with an open crack by observing the changes in natural frequencies is considered to be a popular method in the time domain (Christides and Barr,1984; Narkis,1994; Shen and Pierre,1994; Chondros et.al.,1998; Carneiro and Inman, 2002). These changes are often quite small, the damage location is not detected and the performance is poor in the presence of noise.

Damage detection using spatial data in conjunction with wavelet analysis has found considerable importance of late. The principles behind such wavelet based damage detection relate to the detection of singularities in a function or in any of its derivatives. The locations of the singularities are related to the local extrema of the wavelet coefficients propagating at finer scales in the neighbourhood of the same singularities. The magnitude of the local extrema at the singularity locations relate to the extent of the sudden change in the signal or its derivatives due to the presence of a singularity (Mallat, 2001). Mallat emphasized that although a wavelet transform is able to locate singularities in a signal, there is no certainty of the absence of a rupture of the propagation of maxima at finest scales. In the case of Gaussian wavelets however the non-existence of a rupture

can be guaranteed. Gentile and Messina (2003) carried out a study on wavelet based damage detection focussing mainly on a number of wavelet basis functions including the derivatives of a Gaussian and Symlets. The damage was modelled as an equivalent sub beam having a modified Young's modulus to cater for the sudden change at the damage location. Loutridis et. al. (2004) used Symlet basis function to identify damage in a cracked cantilever beam using a rotational spring damage model. Chang and Chen (2003) and Okafor and Dutta (2000) have considered similar problems concentrating on a single wavelet basis function. Spatial response data from beam structures have been successfully analysed by wavelets to detect damage by Wang and Deng (1999). Advantages of wavelet analysis over the usual eigenvalue analysis for a simply supported beam with non-propagating open crack were shown by Liew and Wang (1998).

It is observed that although the effectiveness of wavelet analysis in damage detection is comparatively well dealt with, most of the works deal with the identification of the location of crack using a single basis function. Very few studies exist on the comparative performance of the wavelet basis functions, windowing and the effects of noise to detect the presence, identify the location and subsequently calibrate the damage. The effects of damage models have not been widely studied either. It is thus felt that there is a necessity of comparing the performance of different wavelet basis functions and damage models for damage detection and calibration in structures incorporating windowing and different levels of presence of noise.

This paper considers a simply supported Euler Bernoulli beam with an open crack. Three damage models of different levels of complexity and details have been considered to simulate the modeshape data. Subsequent analysis of the modeshape using different

wavelet basis functions is performed and the effects of windowing and presence of noise are studied in details. Cracks of different sizes and locations have been used in the examples. An extension of the damage identification for multispan beams is also presented. The effectiveness of a wavelet based damage identification and calibration has been shown considering the variations of the factors stated above.

2. DAMAGE MODELS

2.1 Lumped Crack Model

The lumped crack model is popular among several researchers (Narkis,1994; Okafor and Dutta, 1998; Chang and Chen, 2003; Tian et.al.,2003; Loutridis et.al.,2004; Lam et.al., 2005) looking at the problem of identification of the location of an open crack through wavelet based techniques. The beam with an open crack is modelled as two uncracked beams connected through a rotational spring at the location of crack by assuming that the effects of the crack are applicable in the immediate neighbourhood of the crack location. The length of the beam is L with the damage located at a distance of 'a' from the left hand support of the beam. The crack depth is taken as 'c' and the overall depth of the beam is 'h'. The governing free vibration equation is

$$EI\frac{\partial^4 y}{\partial x^4}+\rho A\frac{\partial^2 y}{\partial t^2}=0 \qquad (1)$$

where E, I, A and ρ are the Young's modulus, the moment of inertia, the cross sectional area and the density of the material of the beam on either side of the crack. The displacement of the beam from its static equilibrium position is y(x,t), at a distance of x from the left hand support along the length of the beam at any time t. Continuity in

displacement, moment and shear are assumed at the location of crack. A slope discontinuity present at the location of the crack and is modelled as

$$\Phi_R'(a) - \Phi_L'(a) = \theta L \Phi_R''(a) \tag{2}$$

where term θ is the non-dimensional crack section flexibility dependent on the crack depth ratio, δ(=a/h). As per Narkis [1], the term θ is considered to be a polynomial of δ as

$$\theta = 6\pi\delta^2(h/L)(0.5033 - 0.9022\delta + 3.412\delta^2 - 3.181\delta^3 + 5.793\delta^4) \tag{3}$$

2.2 Continuous Crack Model

A more detailed and complex continuous crack model is considered following Carneiro and Inman (2002). The model is derived from the stationarity of the Hu-Washizu-Barr functional (Christides and Barr, 1984) and is a refined version of the proposed model by Shen and Pierre (1994) ensuring the self-adjointness of the differential operator for a symmetric matrix representation after the discretization of the free vibration equation. For a rectangular cross section, the stress-strain and the displacement functions are assumed to be locally disturbed in the vicinity of the crack. The effect of the crack is considered maximum at the crack tip and decays exponentially away from it. The stress/strain disturbance function and the displacement disturbance function are

$$f_1(x,z) = [z - m_1(z + c/2)H(h/2 - c - z)]e^{-\alpha_1 \frac{|x-a|}{h/2}} \tag{4}$$

and

$$f_2(x,z) = [z - (z + c/2)H(h/2 - a - z)]e^{-\beta_1 \frac{|x-a|}{h/2}} \tag{5}$$

respectively. The term m_1 is a factor computed considering the continuity of bending moment in the cracked section and α_1 and β_1 are the stress and displacement decay

parameters respectively. The term H(.) is the Heaviside step function. The Cartesian coordinates x , y and z are along the length, breadth and depth of the beam respectively with the origin being at the midpoint of the extreme left hand section. The equation of motion for the free vibration of the beam considering these kinematic assumptions is given as

$$E[p_2(x)\xi(x,t)'']'' + E[p_1(x)\xi(x,t)']' + \rho A\ddot{\xi}(x,t) = 0 \qquad (6)$$

where $\xi(x,t)$ is the vertical displacement of the beam and the primes and overdots represent differentiation with respect to the space and time respectively. The terms $p_1(x)$ and $p_2(x)$ are given in Appendix1.

2.3 Smeared Crack Model

The smeared crack model is relatively simple and considers an open crack reducing the moment of inertia over an affected width. The governing free vibration equation is the same as in equation 1. The damaged beam is analysed as an assembly of three sub-beams, the damaged sub-beam being positioned in between the two undamaged ones. Continuity in deflection, slope, moment and shear are assumed on both left and right ends of the damaged zone. The width of the crack is computed according to the formula by Bovsunovsky and Matveev (2000) as

$$\Delta x = x_2 - x_1 = \frac{0.3675h(1-\delta)}{1-(1-\delta)^3}[(1-\delta)^6 - 3(1-\delta)^2 + 2] \qquad (7)$$

A discontinuity in the modeshape or in any of its derivatives is present in a damaged beam for any model of crack. The first modeshape of the beam with an open crack is simulated as it is convenient to measure the fundamental modeshape for real structures.

3. WAVELET ANALYSIS

The continuous wavelet transform of a square integrable function f(x) can be represented as

$$Wf(b,s) = \int_{-\infty}^{+\infty} f(x) \frac{1}{\sqrt{s}} \psi^*(\frac{x-b}{s}) dx \tag{8}$$

where the wavelet basis function $\psi(x)$ is a zero average function [6] and s and is the b are the scale and the translation parameters respectively. The function $\psi(x)$ also ensures a weak admissibility condition

$$\int_{0}^{+\infty} \frac{|\hat{\psi}(\omega)|^2}{\omega} d\omega < +\infty \tag{9}$$

The identification of a discontinuity in a function or any of its derivatives can be linked with the number of vanishing moments of the wavelet basis function chosen for analysis. For a wavelet with no more than m number of vanishing moments, it can be shown that for very small values of s in the domain of interest, the continuous wavelet transform of a function f(x) can be related to the m^{th} derivative of the signal (Mallat, 2001). The relationship between the continuous wavelet transform of f(x) and its m^{th} derivative can be expressed as

$$\lim_{s\to 0} \frac{Wf(b,s)}{s^{m+1/2}} = K \frac{d^m f(x)}{dx^m} \tag{10}$$

where

$$\int_{-\infty}^{+\infty} \zeta(x) dx = K \neq 0 \tag{11}$$

and $\zeta(x)$ is a function satisfying

$$\psi(x) = (-1)^m \frac{d^m \zeta(x)}{dx^m} \tag{12}$$

Since the simulated first modeshape of a beam with an open crack contains discontinuity in the derivative/s independent of a physically admissible damage model at the location of damage, it is possible to identify the location of the damage through wavelet transform by incorporating a basis function having an appropriate number of vanishing moments (Gentile and Messina, 2003; Pakrashi et.al., 2005).

4. DAMAGE IDENTIFICATION

Damaged modeshape data is simulated and Gaussian white noise is synthetically introduced for a beam of length 1 m. The cross sectional area (A), depth (h) and the moment of inertia (I) of the square beam are taken as 0.0001 m^2, 0.01 m and 8.33×10^{-10} m^4 respectively. The Young's modulus (E) and the density of the beam (ρ) are assumed to be 190×10^9 N/m^2 and 7900 kg/m^3 respectively.

4.1 Basis Independence

The first modeshape was simulated from the lumped crack model for an open crack (δ=0.35) situated at 0.4m from the left hand support and was analyzed using wavelet transform for different wavelet basis functions. Figure 1 shows the results of the analysis for some selected bases. It is observed that as long as the bases satisfy the criterion of the required number of vanishing moments, they can successfully detect the presence and the location of the damage consistently at both fine and coarse scales. Since Haar has only one vanishing moment, a jump of the wavelet coefficients at the location of

the crack is observed instead of a local extremum, as seen incorporating other wavelets with more than one vanishing moment. An analytical expression of the jump size of wavelet coefficients for the current problem using Haar basis has been provided by Pakrashi et al (2005) considering a lumped crack model.

4.2 Model Independence

Figure 2 shows the results of analyzing the same damage using Coif4 wavelet basis function using different damage models. The location of the damage is found irrespective of the model chosen. However, it is observed that the magnitude of the local extremum at the damage location is different for different damage models.

4.3 Windowing

Windowing of the modeshape data and subsequent wavelet analysis improves the damage detection process. Bartlett, Hamming, Hanning, Gaussian and Bohman windows were considered for different damage models and crack depth ratios. The Haar basis is seen to be compatible best with a Bartlett window, while the smoother functions showed very good performance with Hanning window (Figures 3a-3b). The Bartlett window itself has a discontinuity in its first derivative at the midpoint and this leads to a problem of possible non-detection when the damage is near the midpoint. It is not possible to detect a damage if its position is exactly at the midpoint since it is not possible to distinguish between jumps resulting from the presence of a singularity in the window from a singularity present in the signal (Figure 3c).

4.4 Masking

The presence of noise in the modeshape function to be analyzed presents a major difficulty for the damage identification problem. Since the nature of the damage present in the modeshape is similar to that of the noise in terms of singularities present, it is quite difficult to identify the damage in the presence of high noise. The local extremum formed in the wavelet coefficient plot due to the presence of an open crack can get masked partially or completely (Figures 4a-4b). A partial masking is present considering Coif4 basis and Hanning Window in Figure 4a with an edge crack (δ=0.35) situated at 0.1m from the left hand support for a signal to noise ratio (SNR) 95 dB, while a complete masking can be observed for the same crack at 75 dB. Finer scales are affected by masking at a lower SNR than coarser scales.

4.5 Multispan Beams

The effectiveness of a wavelet transform based damage detection problem was extended to asymmetric, multi-span beam structures for a lumped crack model. Selected results from the simulations and subsequent wavelet analysis of two span beams are presented. The cross sectional area and the moment of inertia of the square beam are $1m^2$ and $0.0833m^4$ respectively. The Young's modulus and the density of the beam are assumed to be $23x10^9$ N/m^2 and 2300 kg/m^3 respectively. Coif4 wavelet basis function and Hanning window have been employed for the analysis of the first modeshape.

It is observed that an edge crack situated near the intermediate support is structurally more important than the ones near the two ends of a two span simply supported beam and it is necessary for the wavelet based methodology to identify the

crack near the intermediate support more effectively. Figures 5a-5b consider the first modeshape of a beam with two equal span lengths of 10m. Figure 5a shows successful damage detection for a beam with a crack (δ=0.35) situated 0.5m away from the intermediate support at 75 dB, while in Figure 5b the damage is masked for the same crack situated 0.5m from the left support for the same SNR. A slope discontinuity near the intermediate support affects the modeshape much more than a similar discontinuity near the two ends. As a result, a damage near the intermediate support is detected more efficiently. However, the intermediate support itself also renders a local extremum at its location after wavelet analysis of the modeshape and the magnitude of the extremum can be high enough to undermine the actual damage and lead to a problem of non-detection. A possible solution to this is to window each span separately and perform a wavelet analysis to each partially windowed section.

The possibility of reduced efficiency of damage identification to a considerable extent due to asymmetry in span lengths is studied. The length of the damaged left span is reduced to 5m. Both large and small cracks are considered at a distance of 0.5m from the intermediate support at 90 dB SNR. Crack depth ratios 0.05 and 0.35 are considered and it is observed from Figure 6a-6b that the effect of asymmetric span length does not contribute significantly in terms of damage identification.

5. DAMAGE CALIBRATION

The extent of a local extremum of the wavelet coefficients at the location of damage is an indicator of the extent of damage. However, the calibration does depend on the basis

function, the damage model and the SNR. Examples are presented in this section for the single span beam considered before in this paper.

5.1 Basis Function Dependence and Effects of Noise

A lumped crack is considered at a distance of 0.4m and 0.1m respectively from the left hand side of the simply supported beam. The first windowed (Hanning) modeshape is analyzed using different wavelet basis functions at scale 4 and the crack depth ratios are calibrated against the wavelet coefficient maxima values at the damage location in the presence of noise (Figure 7). The calibration curves for different bases are significantly different and the consistency is affected for small edge cracks in the presence of higher levels of noise because of masking.

5.2 Damage Model Dependence

The same crack with δ=0.35 is identified using Coif4 basis function and Hanning windowing for the crack models presented in this paper for scale 32 (Figures 8.1-8.2). The SNR is considered to be 120dB. The extent of the wavelet coefficient extrema near the damage location is significantly different. The extremum for the smeared crack model is found to be nearly an order lower. The lumped crack model is found to be numerically more efficient and conforms best to the detailed, but numerically most expensive continuous crack beam model.

5.3 Curvature Based Calibration

An alternative way of calibrating damage is by transforming the curvature, rather than the modeshape of the vibrating beam with an open crack. The curvature was numerically

computed from the lumped crack model and a calibration was performed considering scales 4 and 16 with the SNR being at 120 dB for cracks located at 0.1m and 0.4m from the left edge. It is observed that the absolute value and the relative change for a curvature based calibration are better than a calibration based on the modeshape, as shown in Figure 9.

6. CONCLUSION

A wavelet based methodology for detection and calibration of an open crack in beams has been studied in detail numerically. Damage models of various levels of complexity have been considered to model an open crack and the first natural modeshape has been simulated for both single span and multi span beams. It is observed that a wavelet based identification of the location of damage is independent of damage models and basis functions so long as the damage introduces a singularity in the damaged modeshape or in any of its derivatives at the location of the damage and the wavelet bases have a certain number of vanishing moments. Windowing is seen to improve both the identification and calibration of damage location. A case of non-detection due to Bartlett windowing in conjunction with Haar basis function has been identified. The presence of noise in the modeshape data is seen to mask the identification of damage and the finer scales are affected at a higher value of SNR as compared to coarser scales. Structurally important edge crack for multispan beams has been detected successfully. The damage detection using wavelet analysis is seen to be chiefly affected by the position, SNR and the extent of damage. On the other hand, a wavelet based calibration is seen to be additionally dependent on the basis function, scale and the damage models apart from SNR, position

of crack and the extent of crack. Finally, a damage calibration based on curvature values is seen to be more sensitive in comparison with that based on modeshape. This study on wavelet based damage detection and calibration can be helpful for any general open crack problem in structures and provides a guideline for the choice of basis functions and windows. The study also provides a quantitative idea for a reliable and successful calibration due to the presence of noise.

REFERENCES

Bovsunovsky, A.P. and Matveev, V.V. (2000), Analytical Approach to the Determination of Dynamic Characteristics of a Beam with a Closing Crack, *Journal of Sound and Vibration*, 235(3), 415-434

Carneiro, S.H.S and Inman, D.J.(2002), Continuous Model for the Transverse Vibration of Cracked Timoshenko Beams, *Transactions of the ASME, Journal of Vibration and Acoustics*, Vol. 24, 310-320

Chang, C.C., and Chen, L.W. (2003), Vibration Damage Detection of a Timoshenko Beam by Spatial Wavelet Based Approach, *Applied Acoustics*, 64, 1217-1240

Chondros, T.G., Dimarogonas, A.D and Yao, J. A. (1998), Continuous Cracked Beam Vibration Theory, *Journal of Sound and Vibration*, 215(1), 17-34

Christides, S. and Barr, A.D.S.(1984), One-dimensional Theory of Cracked Bernoulli-Euler Beams, *International Journal of Mechanical Sciences*, 26, 639-648

Gentile, A and Messina, A. (2003), On the Continuous Wavelet Transforms Applied to Discrete Vibrational Data for Detecting Open Cracks in Damaged Beams, *International Journal of Solids and Structures*, 40, 295-315

Lam, H.F., Lee, Y.Y., Sun, H.Y., Cheng, G.F., and Guo, X. (2005), Application of the Spatial Wavelet Transform and Bayesian Approach to the Crack Detection of a Partially Obstructed Beam, *Thin Walled Structures*, 43, 1-21

Liew, K.M and Wang, Q. (1998), *Application of Wavelet Theory for Crack Identification in Structures*, ASCE Journal of Engineering Mechanics, February, 152-157

Loutridis, S., Douka, E. and Trochidis, A. (2004), Crack Identification in Double Cracked Beams using Wavelet Analysis, *Journal of Sound and Vibration*, 277, 1025-1039

Mallat, S. (2001), *A Wavelet Tour on Signal Processing*, Academic Press, New York

Narkis, Y. (1994), Identification of Crack Location in Vibrating Simply Supported Beams, *Journal of Sound and Vibration*, 172(4), 549-558

Okafor A.C. and Dutta, A. (2000), Structural Damage Detection in Beams by Wavelet Transforms, *Smart Materials and Structures*, 9, 906-917

Pakrashi, V., Basu, B. and O' Connor, A. (2005), Identification of Open Cracks Using Wavelet Analysis, *Structural Engineering Convention, Bangalore, India,* December 14-16

Shen, M.H.H and Pierre, C.(1994), Free Vibration of Beams with a Single Edge Crack, *Journal of Sound and Vibration*,170(2), 237-259

Tian, J., Li, Z., and Su, X. (2003), Crack Detection in Beams by Wavelet Analysis of Transient Flexural Waves, *Journal of Sound and Vibration*, 2003, 261, 715-727

Wang, Q. and Deng, X. (1999), Damage Detection with Spatial Wavelets, *International Journal of Solids and Structures*, 36, 3443-3468

LIST OF FIGURES

Figure 1. Damage detection for an open crack with different wavelet bases at different scales.

Figure 2. Damage detection for an open crack with different damage models.

Figure 3a. Damage detection using Haar basis in conjunction with Bartlett window.

Figure 3b. Damage detection using fourth derivative of a Gaussian in conjunction with Hanning window.

Figure 3c. A case of non-detection of damage for Haar basis in conjunction with Bartlett window.

Figure 4a. Partial masking of damage due to the presence of low noise.

Figure 4b. Full masking of damage due to the presence of high noise.

Figure 5a. Damage detection in a two span symmetric beam with a crack near the intermediate support.

Figure 5b. Inability of Damage detection in a two span symmetric beam with a crack near the left edge.

Figure 6a. Damage detection for small crack in an asymmetric two span beam.

Figure 6b. Damage detection for a large crack in an asymmetric two span beam.

Figure 7. Effect of noise and Wavelet Bases on wavelet based damage calibration.

Figure 8a. Dependence of damage models for a wavelet based damage calibration at finer (scale 4) scales.

Figure 8b. Dependence of damage models for a wavelet based damage calibration at coarser (scale 32) scales.

Figure 9. Wavelet based damage calibration on computed curvature of damaged beam with an open crack.

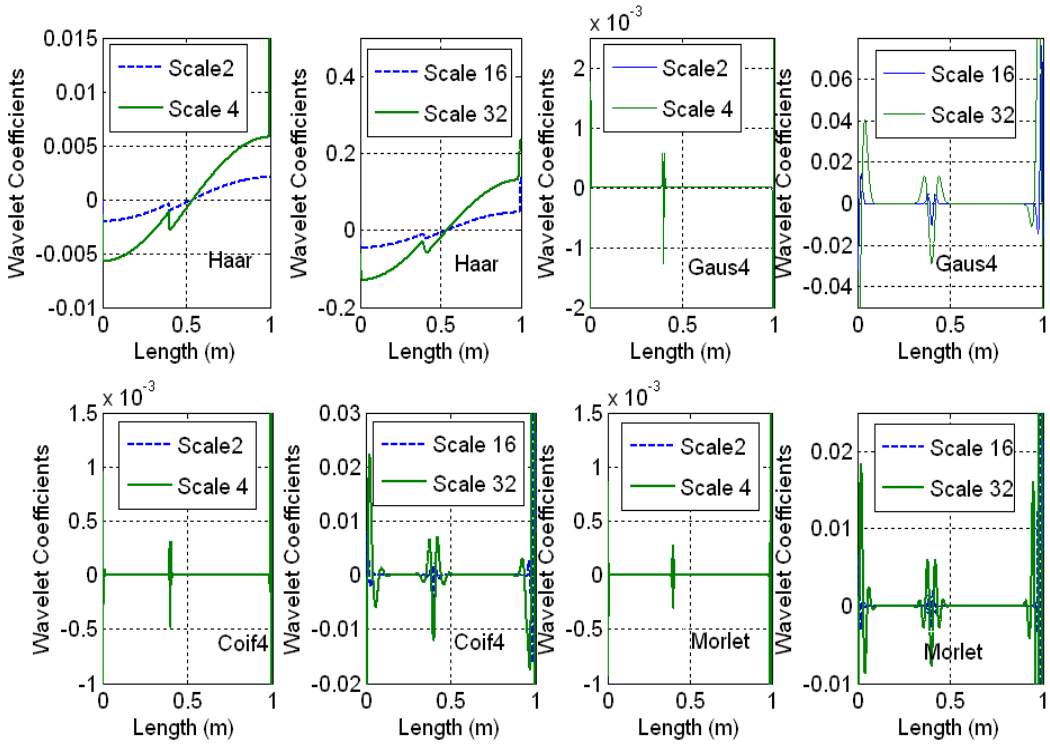

Scale2
Scale 4
Haar
Scale 16
Scale 32
Haar
Scale2
Scale 4
Gaus4
Scale 16
Scale 32
Gaus4
Scale2
Scale 4
Coif4
Scale 16
Scale 32
Coif4
Scale2
Scale 4
Morlet
Scale 16
Scale 32
Morlet
Wavelet Coefficients
Length (m)
x 10^-3

Figure 1.

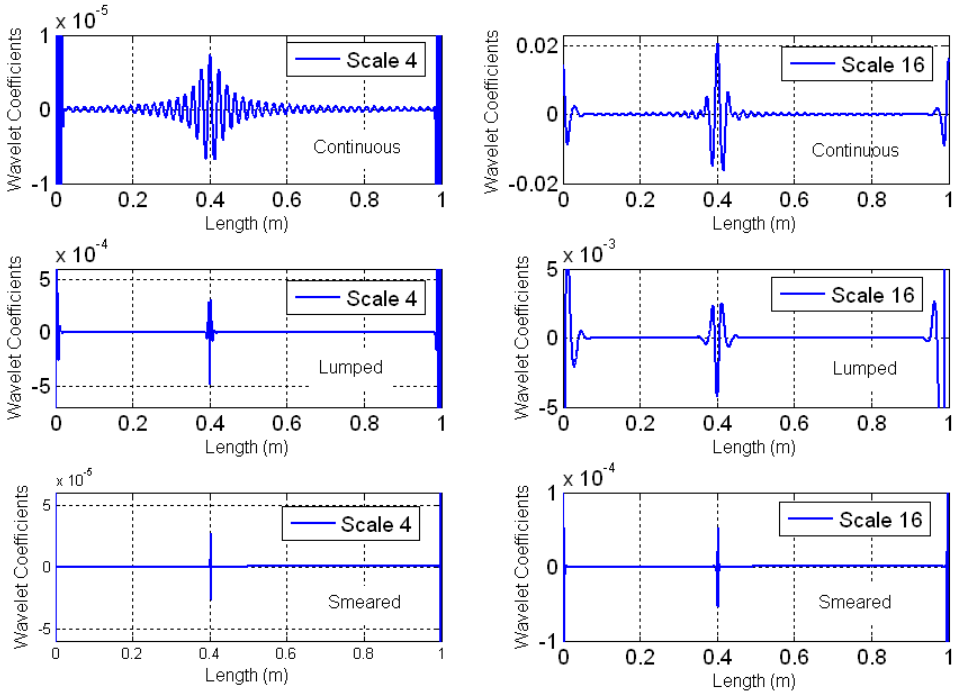

x 10^-5
Wavelet Coefficients
Scale 4
Continuous
Length (m)
Scale 16
Continuous
Length (m)
x 10^-4
Scale 4
Lumped
Length (m)
x 10^-3
Scale 16
Lumped
Length (m)
x 10^-5
Scale 4
Smeared
Length (m)
x 10^-4
Scale 16
Smeared
Length (m)

Figure 2.

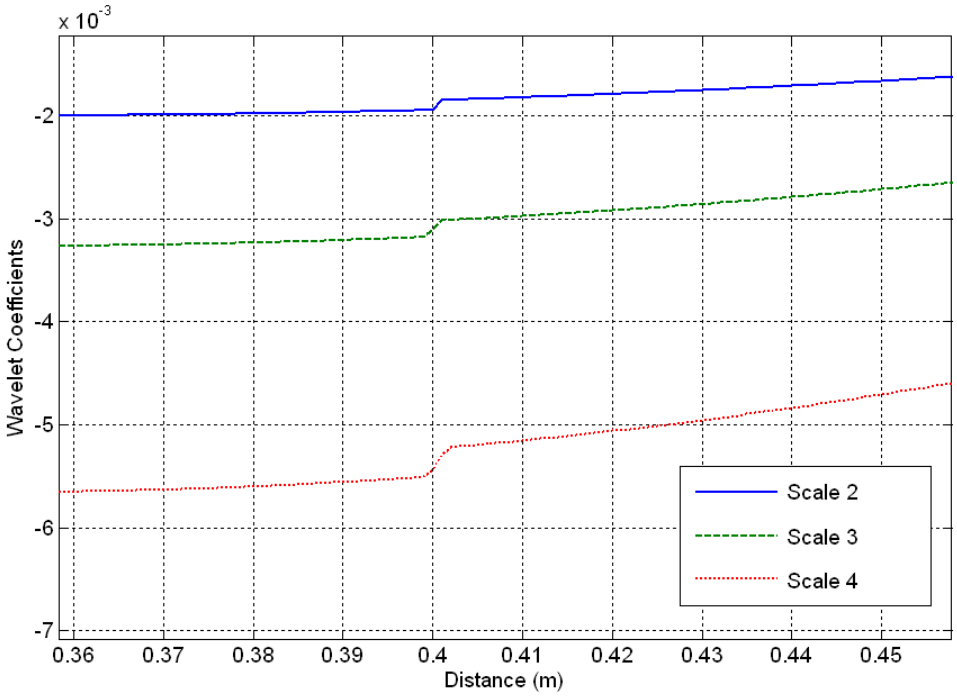

x 10^-3
-2
-3
-4
-5
-6
-7
Wavelet Coefficients
0.36
0.37
0.38
0.39
0.4
0.41
0.42
0.43
0.44
0.45
Distance (m)
Scale 2
Scale 3
Scale 4

Figure 3a.

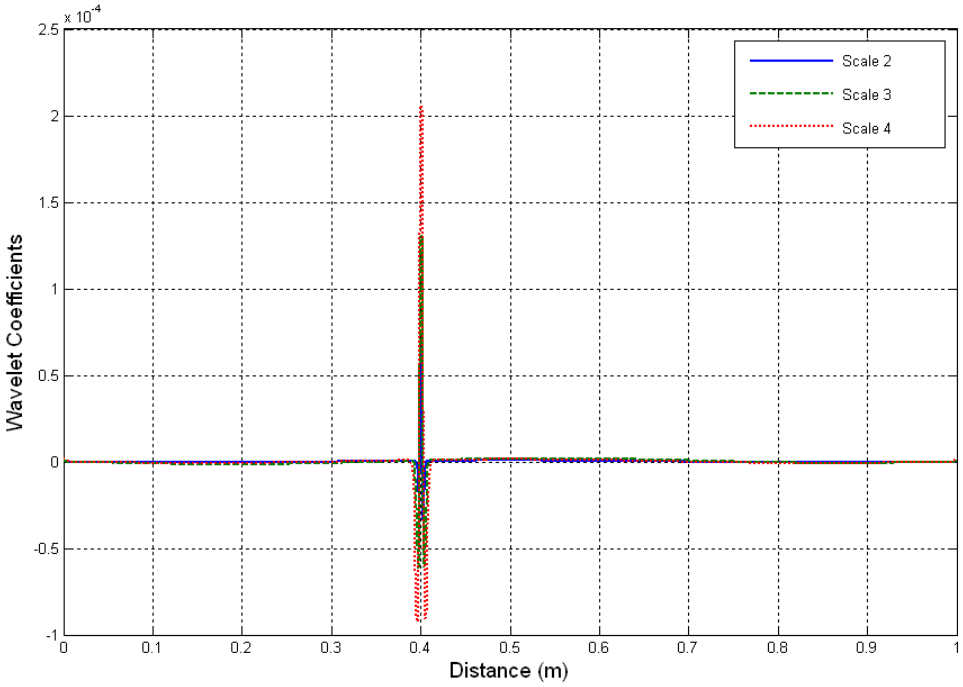

x 10^-4
2.5
2
1.5
1
0.5
0
-0.5
-1
Wavelet Coefficients
0
0.1
0.2
0.3
0.4
0.5
0.6
0.7
0.8
0.9
1
Distance (m)
Scale 2
Scale 3
Scale 4

Figure 3b.

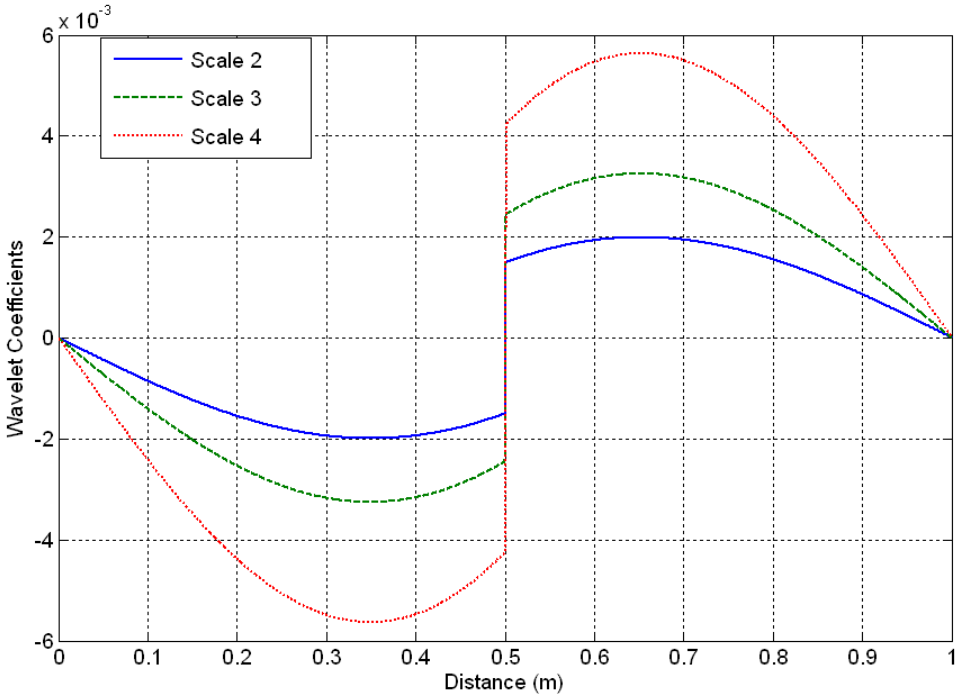

x 10^-3
Scale 2
Scale 3
Scale 4
Wavelet Coefficients
Distance (m)
6
4
2
0
-2
-4
-6
0
0.1
0.2
0.3
0.4
0.5
0.6
0.7
0.8
0.9
1

Figure 3c.

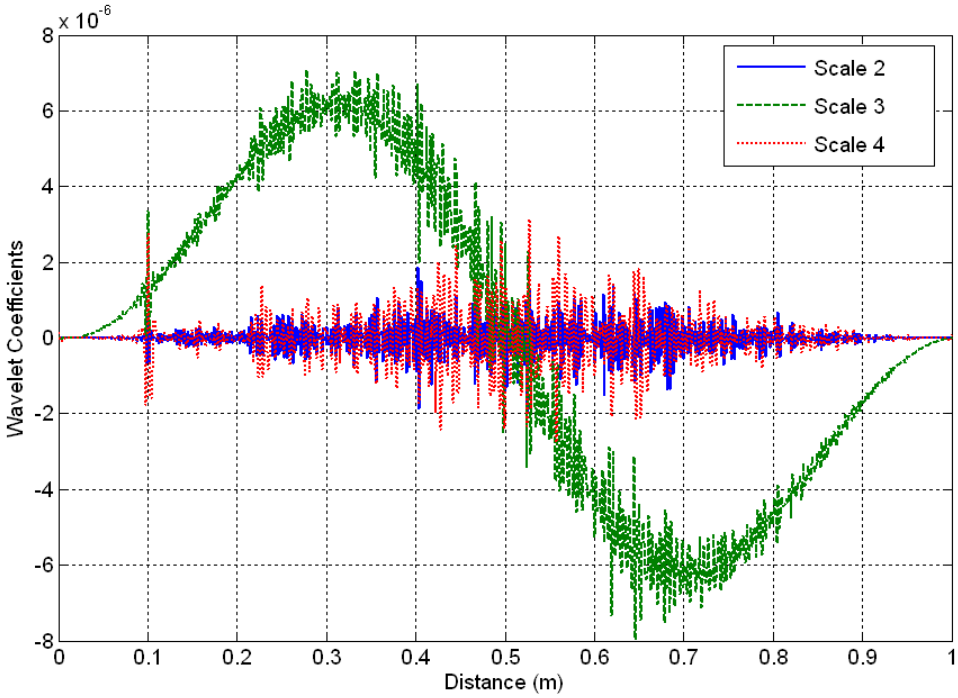

x 10^-6
8
6
4
2
0
-2
-4
-6
-8
Wavelet Coefficients
0
0.1
0.2
0.3
0.4
0.5
0.6
0.7
0.8
0.9
1
Distance (m)
Scale 2
Scale 3
Scale 4

Figure 4a.

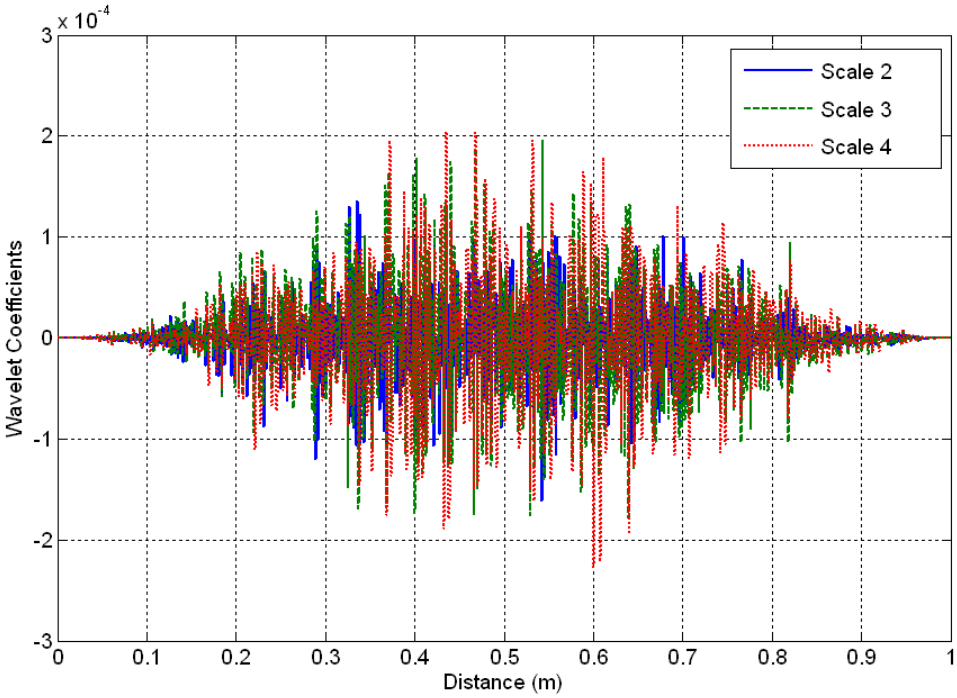

x 10^-4
3
2
1
0
-1
-2
-3
Wavelet Coefficients
0
0.1
0.2
0.3
0.4
0.5
0.6
0.7
0.8
0.9
1
Distance (m)
Scale 2
Scale 3
Scale 4

Figure 4b.

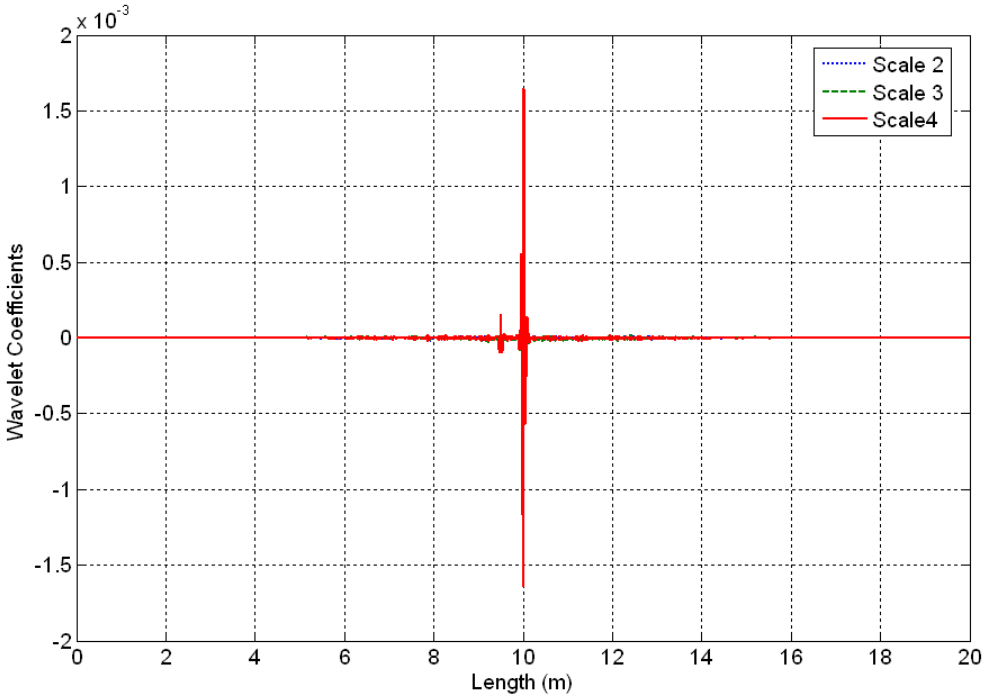

x 10^-3
2
1.5
1
0.5
0
-0.5
-1
-1.5
-2
0
2
4
6
8
10
12
14
16
18
20
Wavelet Coefficients
Length (m)
Scale 2
Scale 3
Scale4

Figure 5a.

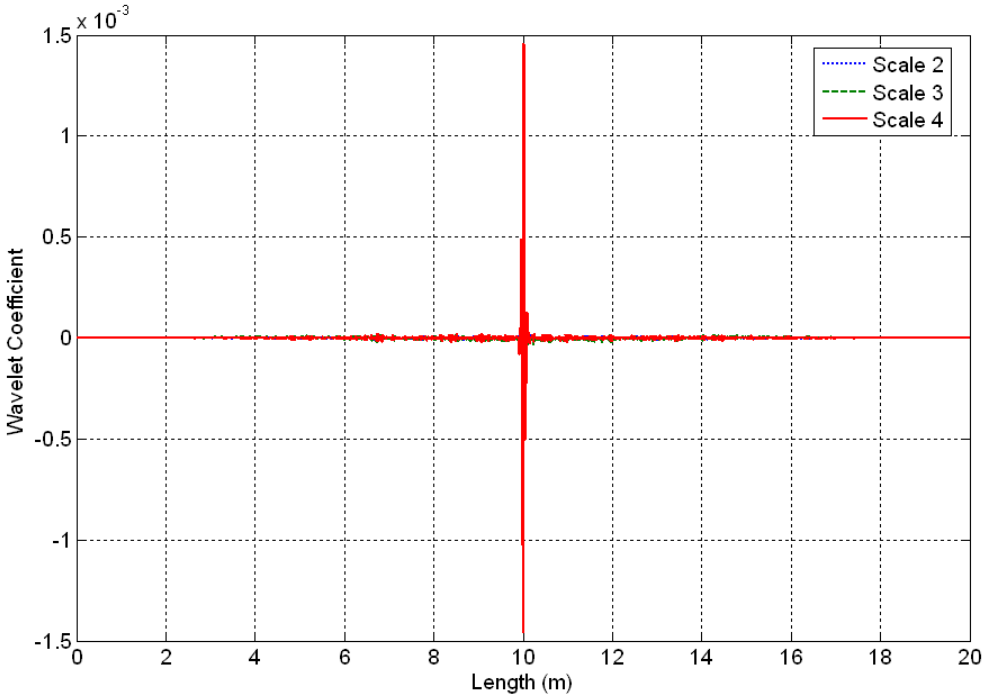

x 10^-3
1.5
1
0.5
0
-0.5
-1
-1.5
Wavelet Coefficient
0
2
4
6
8
10
12
14
16
18
20
Length (m)
Scale 2
Scale 3
Scale 4

Figure 5b.

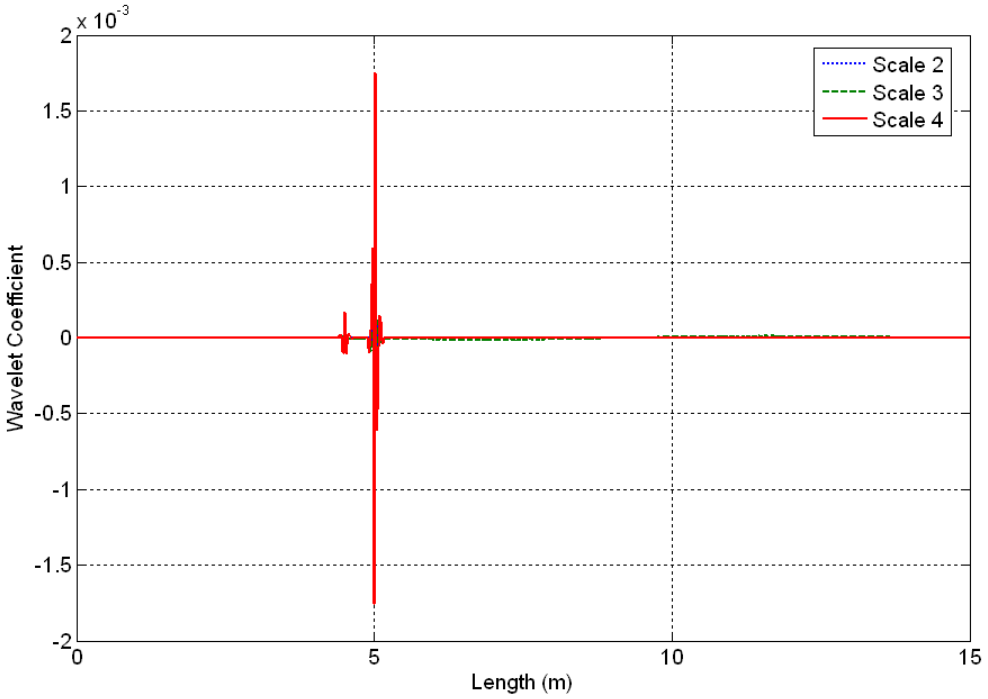

x 10^-3
2
1.5
1
0.5
0
-0.5
-1
-1.5
-2
0
5
10
15
Length (m)
Wavelet Coefficient
Scale 2
Scale 3
Scale 4

Figure 6a.

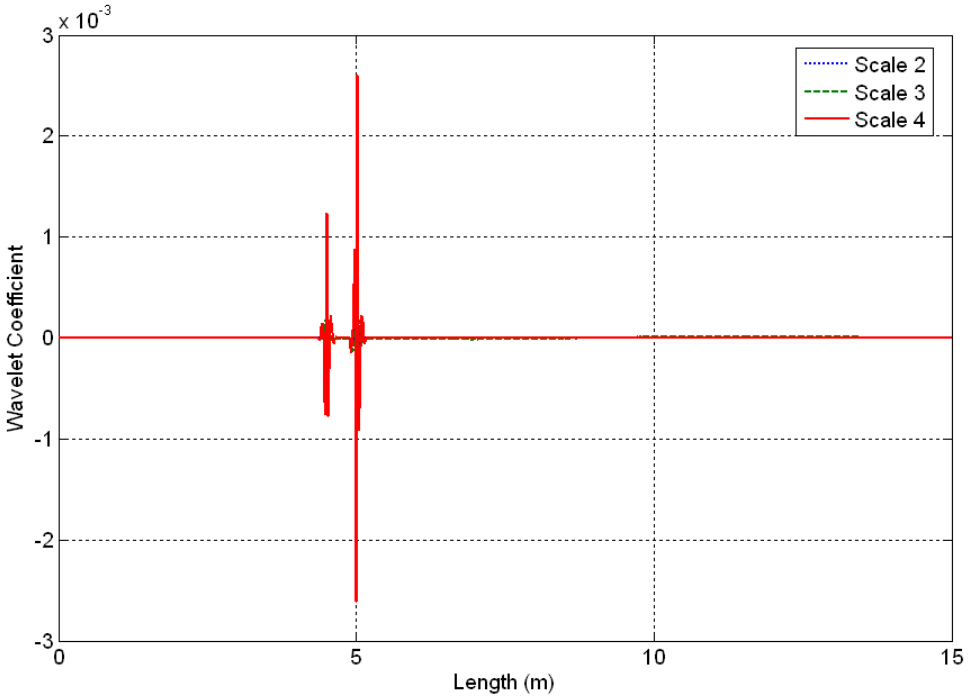

x 10^-3
3
2
1
0
-1
-2
-3
Wavelet Coefficient
0
5
10
15
Length (m)
Scale 2
Scale 3
Scale 4

Figure 6b.

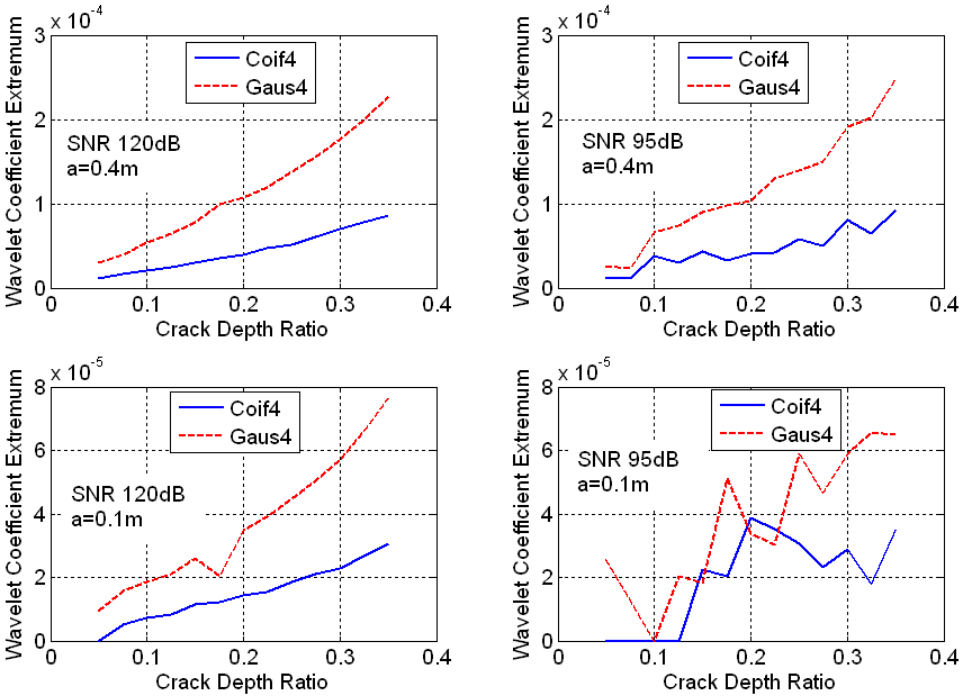

x 10^-4
Wavelet Coefficient Extremum
Coif4
Gaus4
SNR 120dB
a=0.4m
Crack Depth Ratio
x 10^-4
Wavelet Coefficient Extremum
Coif4
Gaus4
SNR 95dB
a=0.4m
Crack Depth Ratio
x 10^-5
Wavelet Coefficient Extremum
Coif4
Gaus4
SNR 120dB
a=0.1m
Crack Depth Ratio
x 10^-5
Wavelet Coefficient Extremum
Coif4
Gaus4
SNR 95dB
a=0.1m
Crack Depth Ratio

Figure 7.

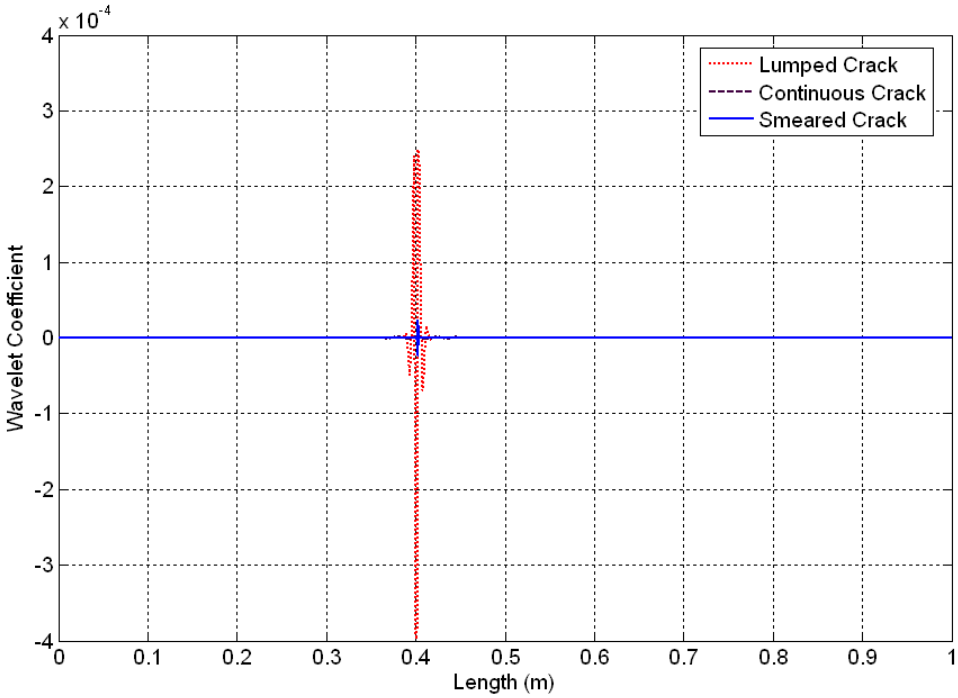

x 10^-4
4
3
2
1
0
-1
-2
-3
-4
Wavelet Coefficient
0
0.1
0.2
0.3
0.4
0.5
0.6
0.7
0.8
0.9
1
Length (m)
Lumped Crack
Continuous Crack
Smeared Crack

Figure 8a.

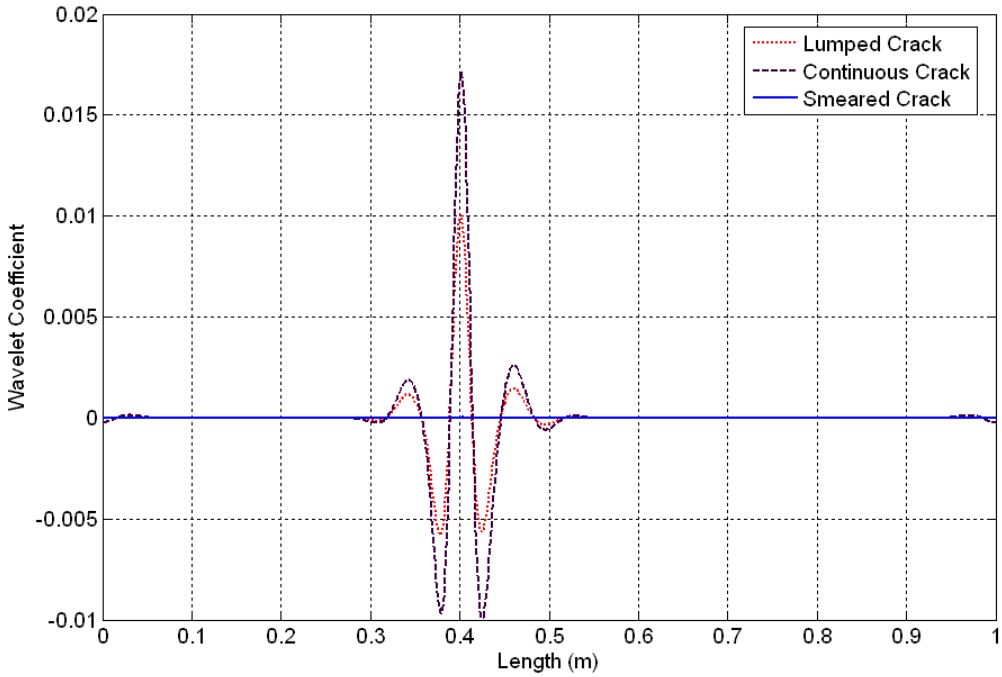

Lumped Crack
Continuous Crack
Smeared Crack
Wavelet Coefficient
Length (m)
0.02
0.015
0.01
0.005
0
-0.005
-0.01
0
0.1
0.2
0.3
0.4
0.5
0.6
0.7
0.8
0.9
1

Figure 8b.

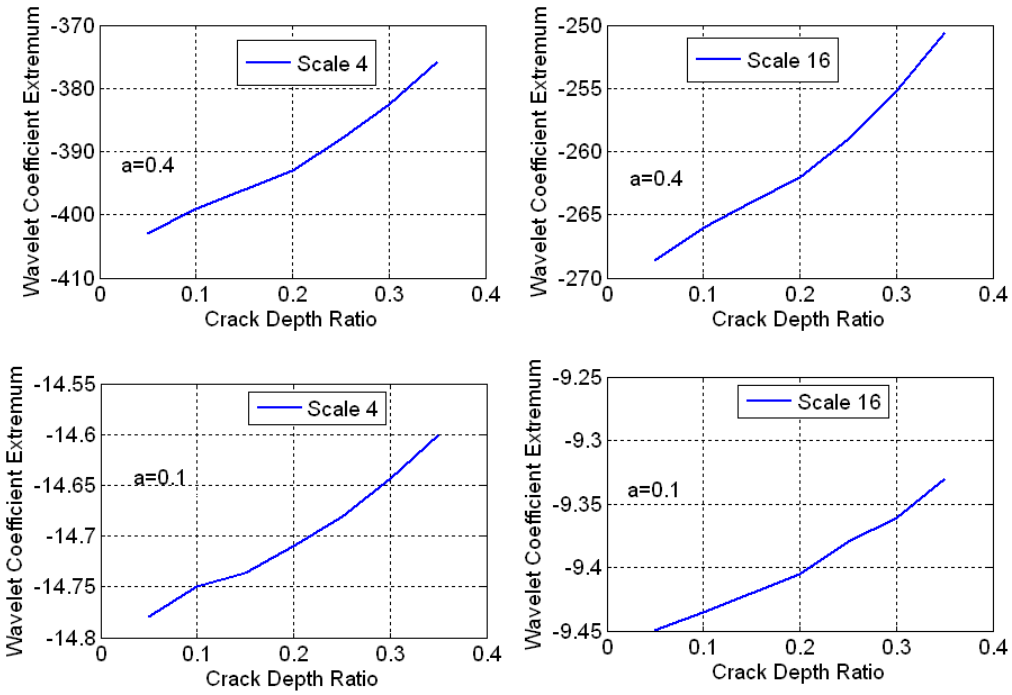

Wavelet Coefficient Extremum
-370
-380
-390
-400
-410
Scale 4
a=0.4
0
0.1
0.2
0.3
0.4
Crack Depth Ratio
Wavelet Coefficient Extremum
-250
-255
-260
-265
-270
Scale 16
a=0.4
0
0.1
0.2
0.3
0.4
Crack Depth Ratio
Wavelet Coefficient Extremum
-14.55
-14.6
-14.65
-14.7
-14.75
-14.8
Scale 4
a=0.1
0
0.1
0.2
0.3
0.4
Crack Depth Ratio
Wavelet Coefficient Extremum
-9.25
-9.3
-9.35
-9.4
-9.45
Scale 16
a=0.1
0
0.1
0.2
0.3
0.4
Crack Depth Ratio

Figure 9.

APPENDIX 1. COEFFICIENTS $p_1(X)$ AND $p_2(X)$ FOR THE CONTINUOUS CRACKED MODEL

$$p_1(x) = E[\{I - \int_A zf_1(x,z)dA - \int_A zf_2(x,z)dA + \int_A f_1(x,z)f_2(x,z)dA\}(\frac{\int_A f_1(x,z)f_2'(x,z)dA) - (\int_A zf_2(x,z)dA)'}{I - 2\int_A zf_1(x,z)dA + \int_A f_1^{\,2}(x,z)dA})' +$$

$$\{(\int_A f_2(x,z)f_1'(x,z)dA))' - (\int_A zf_1(x,z)dA)''\}(\frac{\int_A f_1(x,z)f_2'(x,z)dA) - (\int_A zf_2(x,z)dA)'}{I - 2\int_A zf_1(x,z)dA + \int_A f_1^{\,2}(x,z)dA})]$$

(A1)

$$p_2(x) = [I - \int_A zf_1(x,z)dA - \int_A zf_2(x,z)dA + \int_A f_1(x,z)f_2(x,z)dA](\frac{I - \int_A zf_1(x,z)dA - \int_A zf_2(x,z)dA + \int_A f_1(x,z)f_2(x,z)dA}{I - 2\int_A zf_1(x,z)dA + \int_A f_1^{\,2}(x,z)dA})$$

(A2)